Molecular Pharmacology Fast Forward. Published on December 6, 2005 as doi:10.1124/mol.105.017715
This article has not been copyedited and formatted. The final version may differ from this version.

MOL 17715

A MEMBRANE-PERMEABLE PEPTIDE CONTAINING THE LAST 21 RESIDUES OF $G\alpha_S$ CARBOXYL TERMINUS INHIBITS G_S COUPLED RECEPTOR SIGNALING IN INTACT CELLS.

Correlations between peptide structure and its biological activity.

Anna Maria D'Ursi[1], Laura Giusti[1], Stefania Albrizio, Francesca Porchia, Cinzia Esposito, Gabriella Caliendo, Claudia Gargini, Ettore Novellino, Antonio Lucacchini, Paolo Rovero and Maria Rosa Mazzoni.

Dipartimento di Psichiatria, Neurobiologia, Farmacologia e Biotecnologie (C.G., L.G., A.L., M.R.M., F.P.), Università di Pisa, Pisa, Italy.

Dipartimento di Scienze Farmaceutiche (A.M.D., C.E.), Università di Salerno, Fisciano (Sa), Italy.

Dipartimento di Chimica Farmaceutica e Tossicologica (S.A., G.C., E.N.), Università di Napoli "Federico II", Napoli, Italy.

Laboratorio di Chimica e Biologia di Peptidi e Proteine, Dipartimento di Scienze Farmaceutiche (P.R.), Università di Firenze, Sesto Fiorentino (Fi), Italy.

Molecular Pharmacology Fast Forward. Published on December 6, 2005 as DOI: 10.1124/mol.105.017715
This article has not been copyedited and formatted. The final version may differ from this version.

MOL 17715

Running Title: Disruption of receptor signaling by a cell-penetrating peptide.

Corresponding author: Maria R. Mazzoni, M.D.
Dip. di Psichiatria, Neurobiologia,
Farmacologia e Biotecnologie
Via Bonanno 6
56126 Pisa, Italy.
Tel. +39-050-2219524
FAX +39-050-2219609
e-mail: mariarm@farm.unipi.it

Number of text pages: 40

Number of tables: 1

Number of figures: 8

Number of references: 40

Number of the words in the Abstract: 250

Number of the words in the Introduction: 626

Number of the words in the Discussion: 1942

ABBREVIATIONS: GPCR, G protein coupled receptor; $G\alpha_s(374\text{-}394)C^{379}A$, a synthetic peptide corresponding to those residues of $G\alpha_s$ with a cysteine substituted by an alanine; DQF-COSY, double-quantum filter correlation spectroscopy; TOCSY, total correlation spectroscopy; NOESY, nuclear Overhauser spectroscopy; DPC, dodecyl phosphocholine; DPPC, dipalmitoyl phosphatidyl cholin; TAT, transactivating regulatory protein; MPS, Kaposi fibroblast growth factor signal sequence.

Molecular Pharmacology Fast Forward. Published on December 6, 2005 as DOI: 10.1124/mol.105.017715
This article has not been copyedited and formatted. The final version may differ from this version.

ABSTRACT

Cell-penetrating peptides are able to transport covalently attached cargoes such as peptide or polypeptide fragments of endogenous proteins across cell membranes. Taking advantage of the cell-penetrating properties of the 16 residue fragment penetratin, we synthesized a chimeric peptide that posses a N-terminal sequence with membrane penetrating activity and a C-terminal sequence corresponding the last 21 residues of $G\alpha_s$. This $G\alpha_s$ peptide was an effective inhibitor of 5'-N-ethylcarboxamidoadenosine (NECA) and isoproterenol stimulated production of cAMP in rat PC12 and human microvascular endothelial (HMEC-1) cells while the carrier peptide had no effect. The maximal efficacy of NECA was substantially reduced when PC12 cells were treated with the chimeric peptide suggesting that it competes with $G\alpha_s$ for interaction with receptors. The peptide inhibited neither G_q nor G_i coupled receptor signaling. The use of a carboxy-fluorescein derivative of the peptide proved its ability to cross plasma membrane of live cells. NMR analysis of the chimeric peptide structure in a membrane mimicking environment showed that the $G\alpha_s$ fragment assumed an amphipathic α-helical conformation tailored to make contact with key residues on the intracellular side of the receptor. The N-terminal penetratin portion of the molecule also showed an α-helical structure but hydrophobic and hydrophilic residues formed clustered surfaces at the N-terminus and center of the fragment suggesting their involvement in the mechanism of penetratin internalization by endocytosis. Our biological data supported by NMR analysis indicate that the membrane-permeable $G\alpha_s$ peptide is a valuable, non-toxic research tool to modulate G_s-coupled receptor signal transduction in cell culture models.

Molecular Pharmacology Fast Forward. Published on December 6, 2005 as DOI: 10.1124/mol.105.017715
This article has not been copyedited and formatted. The final version may differ from this version.

INTRODUCTION

G protein coupled receptors (GPCRs) represent a large family of cell surface receptors sharing a common transmembrane structure and signal transduction mechanisms. The basic unit of GPCR signaling is composed by a heptahelical receptor, a heterotrimeric GTP-binding protein (G protein) and an effector such as an enzyme or an anion channel. The binding of an agonist ligand to the GPCR changes its conformation so to allow productive coupling with its cognate G protein, leading to the exchange of GTP for GDP on the Gα subunit and consequent dissociation of Gα-GTP from the Gβγ complex.

Multiple sites of interaction cooperate in the physical coupling between the activated receptor and the G protein (reviewed by: Cabrera-Vera et al., 2003). Data from crystallographic, biochemical and mutagenesis studies indicate that the key elements of the interaction are primarily the second and third intracellular loops of the receptor making physical contact with the C-terminus of the Gα subunit ((Kobilka et al., 1988; Kostenis et al., 1997). The last ~50 residues of Gα subunits play a central role in discriminating between different receptor subtypes or different functional states of the same receptor (Havlickova et al., 2003; Slessareva et al., 2003; Cabrera-Vera et al., 2003).

Pharmacologic agents that act as agonists or antagonists of GPCRs are the most common type of drug in clinical use today. Irrespective of their chemical structure, all these agents have a common mechanism of action in that they act extracellularly either to mimic or to preclude agonist binding to its receptor. As alternative approach to

Molecular Pharmacology Fast Forward. Published on December 6, 2005 as DOI: 10.1124/mol.105.017715
This article has not been copyedited and formatted. The final version may differ from this version.

antagonism of GPCR signaling, the receptor-G protein interface can be targeted with agents that block coupling between the receptor and G protein intracellularly. Such approach is expected to produce G protein-specific, rather than receptor specific, antagonism. This strategy has produced several successful results using polypeptides derived from either the putative contact surface on the receptor or the Gα subunit (reviewed by: Freissmuth et al., 1999).

In intact cells, membrane-permeable peptides containing the C-terminal sequence of $G\alpha_q$ and $G\alpha_s$ disrupt 5-HT_{2c} and β_2 adrenergic receptor-mediated activation of phospholipase C-β (PLC-β) and adenylyl cyclase, respectively (Chang et al., 2000). Cellular expression of a 83 residue polypeptide derived from C-terminus of $G\alpha_s$ inhibits β_2 adrenergic and dopamine D_{1A} receptor-mediated cAMP production (Feldman et al., 2002). Minigene plasmids encoding oligopeptides representing the last 11 C-terminal residues of $G\alpha_i$, $G\alpha_o$, $G\alpha_q$, $G\alpha_{12}$ and $G\alpha_{13}$ have been successfully used to discern the contribution of different G proteins to signaling by M_2 muscarinic and thrombin receptors (Gilchrist et al., 1999; Vanhauwe et al., 2002).

In a previous paper (Mazzoni et al., 2000), we have shown that a 21 residue synthetic peptide, $G\alpha_s(374\text{-}394)C^{379}A$, derived from rat $G\alpha_s$ C-terminus inhibits A_{2A} adenosine receptor-mediated activation of adenylyl cyclase in rat striatal membranes and it acquires a defined helical conformation in solution. Here, we present both biological and structural data of a membrane-permeable synthetic peptide containing the sequence of the $G\alpha_s(374\text{-}394)C^{379}A$ peptide on the C-terminal side. This membrane-permeable peptide was designed using as carrier molecule, penetratin, a 16 residue fragment derived

from the homeodomain of the *Drosophila* transcription factor Antennapedia that translocates through biological membranes (Derossi et al., 1994). The membrane-permeable 37 residue peptide (dubbed A42) was able to cross HMEC-1 and PC12 cell plasma membrane inhibiting A_{2A}, A_{2B} adenosine and β-adrenergic receptor stimulated cAMP production without affecting G_q and G_i coupled receptor signaling. Structural data pointed out the molecular basis of A42 tropism for plasma membrane. According to previous conformational studies of isolated penetratin (Lindberg et al., 2001) and $G\alpha_s$ fragments (Mazzoni et al., 2000) both A42 segments were arranged in α-helical structures so that the presence of one did not affect the conformation and functionality of the other. Our synthetic peptide represents a powerful tool to inhibit G_s coupled receptor signaling in intact cells.

MATERIALS AND METHODS

Adenosine deaminase was obtained from Roche Molecular Biochemicals (Mannheim, Germany). Fetal bovine serum (FBS) was from Cambrex Corporation (East Rutherford, NJ). MCDB 131 medium was purchased from Invitrogen Corporation (Carlsbad, CA). Kaighn's modified Ham's F12 medium (F12K), penicillin, streptomycin, horse serum (HS), papaverine, 5'-N-ethylcarboxamidoadenosine (NECA), isoproterenol, forskolin and direct cAMP enzyme immunoassay kit (CA-200) were products of Sigma-Aldrich Inc. (St. Louis, MO). 2,4-Difluoro-α-α^1-bis(1H-1,2,4–triazol-1ylmethyl)benzyl alcohol (fluconazole) was a product of Pfizer (New York, NY). All other reagents were from standard commercial sources and of the highest grade available.

Molecular Pharmacology Fast Forward. Published on December 6, 2005 as DOI: 10.1124/mol.105.017715
This article has not been copyedited and formatted. The final version may differ from this version.

Cell Culture

PC12 cells obtained from the American Type Culture Collection (Rockville, MD) were maintained in F12K medium supplemented with 15% HS, 2.5% FBS, 100 units/ml penicillin, 100 μg/ml streptomycin and 0.02 mg/ml fluconazole in an atmosphere of 95% air, 5% CO_2 at 37°C. Cells were recultivated 2-3 times per week. A human dermal microvascular endothelial cell line that was transformed using SV-40 was also used (HMEC-1; obtained from Dr. E. Ades (Centers for Disease Control, Atlanta, GA). Cells were maintained in MCDB 131 medium supplemented with 5% FBS, penicillin/streptomycin (5000 units/ml; 5000 μg/ml), hydrocortisone (500 μg/ml), epidermal growth factor (0.01 μg/ml), and L-glutamine (2 mM) at 37ºC as above. Cells were seeded at 1 x 10^5 cells/ml and subcultured at confluency. In our studies, cells were used at passages 18-24.

To determine the number of viable PC12 cells in proliferation, a colorimetric assay was used (CellTiter 96® AQ_{ueous} One Solution Cell Proliferation Assay; Promega Corporation, Madison, WI). PC12 cells were seeded in a 96 well plate (6 x 10^3 cells/well) and maintained in culture for 48 h changing medium after 24 h. The A42 peptide was added at a final concentration of 300 μM and incubated for 30 min at 37°C. At the end of this period the CellTiter 96® AQ_{ueous} One Solution Reagent was added according to the manufacturer instruction and the plate was incubated in the dark for 2 h at 37°C. Absorbance was recorded at 490 nm using a Wallac 1420 multilabel counter (PerkinElmer, Inc., Boston, MA).

Molecular Pharmacology Fast Forward. Published on December 6, 2005 as DOI: 10.1124/mol.105.017715
This article has not been copyedited and formatted. The final version may differ from this version.

To obtain PC12 differentiation into sympathetic-like neurons, cells were seeded in 8 well Poly-D-Lysin coated culture slides (3,000 cells/well) and cultured in the presence of 100 ng/ml of fibroblast growth factor (FGF) for 5 days. The culture medium containing FGF was replaced every 2 days. Before treatment with the fluorescein labeled peptide, cells were rinsed twice with 8.1 mM Na_2HPO_4, 1.5 mM KH_2PO_4, pH 7.4, 136.8 mM NaCl, 2.7 mM KCl (PBS) containing 0.5 mM $MgCl_2$ and 0.6 mM $CaCl_2$ (DPBS) and then incubated in serum free F12K medium containing 1 mg/ml bovine serum albumin (BSA) in the presence and absence of 100 μM fluorescent A42 peptide for 30 min, 3 and 6 h. At the end of the incubation times, cells were rinsed twice with DPBS and treated with the Image-iT™Live Plasma Membrane and Nuclear Labeling Kit (Molecular Probes, Carlsbad, CA) according to the manufacturer instruction. Fluorescent specimens were viewed using a Zeiss Axioskop microscope. Digital images were taken with a Leica DC100 camera. The brightness and the contrast of the final images were adjusted using Adobe Photoshop (Version 6.00).

Peptide Synthesis

Peptides were synthesized manually, using a conventional solid-phase strategy based on the Fmoc/t-Bu protection chemistry. The crude products were purified to homogeneity by semi-preparative HPLC. The final peptides were characterized by analytical HPLC (purity > 98%) and mass spectrometry. Peptide sequences are as follow: H-Arg-Gln-Ile-Lys-Ile-Trp-Phe-Gln-Asn-Arg-Arg-Met-Lys-Trp-Lys-Lys for the carrier peptide (A40) and H-Arg-Gln-Ile-Lys-Ile-Trp-Phe-Gln-Asn-Arg-Arg-Met-Lys-Trp-Lys-Ly-Arg-Val-Phe-Asn-Asp-Ala-Arg-Asp-Ile-Ile-Gln-Arg-Met-His-Leu-Arg-Gln-

Molecular Pharmacology Fast Forward. Published on December 6, 2005 as DOI: 10.1124/mol.105.017715
This article has not been copyedited and formatted. The final version may differ from this version.

Tyr-Glu-Leu-Leu-OH (A42) for the membrane-permeable $G\alpha_s$ peptide (the $G\alpha_s$ C-terminal sequence is underlined). A fluorescent analogue of A42 was prepared by EspKem (Florence, Italy), linking carboxy-fluorescein to the peptide N-terminus, spaced by a residue of ω-amino butiric acid.

Peptides were dissolved in water to obtain 2 mM stock solutions. All peptide stock solutions were centrifuged at 11,000*g* for 4 min at room temperature and supernatants collected. The concentration of the membrane-permeable $G\alpha_s$ peptide was roughly estimated spectrophotometrically using the molar extinction coefficient for tyrosine at 280 nm (ε_{280nm} = 1400 M^{-1} cm^{-1}) as reported previously (Mazzoni et al., 2000).

Measurement of Intracellular cAMP

To study receptor mediated cAMP accumulation, PC12 cells (passages 6-18) or HMEC-1 (passage 18-24) were seeded in 24 wells culture plates at the density about 6 x 10^4 or 1 x 10^5 cells/well and used just after reaching confluence. Cells were preincubated in the presence of 100 μM papaverine with and without 1 unit/ml of adenosine deaminase in F12K or MCDB 131 medium for 30 min at 37°C. Assays were initiated by the addition of 1 μM (PC12), 5 μM (HMEC-1) NECA or 1 μM (HMEC-1) isoproterenol followed by incubation for 15 min at 37°C. Peptides (A40 or A42) were added 30 min before assay initiation together with papaverine. At the end of the incubation time, the reaction was terminated by removal of the reaction medium, followed immediately by the addition of 0.3 ml of 0.1 N HCl. The HCl extracts were collected into 15 ml Falcon tubes and cells were rinsed with an additional 0.3 ml of 0.1 N HCl. Samples of the pooled HCl extract where centrifuged at 600*g* for 10 min. Aliquots (100 μl) of the supernatant were

Molecular Pharmacology Fast Forward. Published on December 6, 2005 as DOI: 10.1124/mol.105.017715
This article has not been copyedited and formatted. The final version may differ from this version.

processed to measured cAMP content using the direct cAMP enzyme immunoassay kit of Sigma-Aldrich Inc.

The effect of A42 on the concentration response curve of NECA (0.1 nM to 5 μM) was evaluated pre-incubating PC12 cells in the presence and absence of 10, 50 and 100 μM A42. The concentration-dependent effect of A42 was evaluated by pre-incubating PC12 cells with eleven different concentrations of the peptide ranging from 0.05 to 560 μM.

To study the effect of the membrane permeable $G\alpha_s$ peptide on adenylyl cyclase and G_i signaling, PC12 cells were preincubated in the presence of 100 μM papaverine with and without 100 μM A42 in F12K medium for 30 min at 37°C. At the end of the preincubation period, either 10 μM forskolin, 1 μM ADPβS ($P2y_{12}$ receptor agonist) or both were added and incubated for 15 min at 37°C. Thereafter, the incubation medium was removed, 0.1 N HCl was added and samples were processed as described above.

Measurement of Intracellular Calcium

Measurement of $[Ca^{2+}]_i$ was performed as previously described (Ceccarelli et al., 2003). Briefly, confluent PC12 cells cultured in 24 well plates were incubated with and without 100 μM A42 in loading buffer (20 mM HEPES, pH 7.4, 130 mM NaCl, 5 mM KCl, 2 mM $CaCl_2$, 1 mM $MsSO_4$, 0.8 mM Na_2HPO_4, 0.2 mM NaH_2PO_4, 25 mM mannose and 1 mg/ml BSA) containing 2 μM Fluo-3 acetoxymethyl ester (Fluo-3 AM) and 0.008% Pluronic F-127 for 30 min at 37°C. After incubation, cells were rinsed with detaching buffer (10 mM HEPES, pH 7.4, 140 mM NaCl, 5 mM KCl, 0.55 mM $MgCl_2$ and 3 mM EDTA) and incubated in the same buffer for 10 min at 37°C. Detached cells

were harvested by low speed centrifugation (1000 g), resuspended in assay buffer (10 mM HEPES, pH 7.4, 140 mM NaCl, 5 mM KCl, 0,55 mM $MgCl_2$ and 1 mM $CaCl_2$) and analysed on a FACScan flow cytometer with the CellQuest software (Becton Dickinson Labware).

To study receptor mediated increase of $[Ca^{2+}]_i$, sample basal fluorescence was measured and then 100 μM ATPγS (P2y2 receptor agonist) was added. The cell flow was halted during this addition and sample measurement was carried out within 2-3 s.

Data Analysis

Data from concentration-response curves were analyzed by a least-squares curve-fitting computer program (GraphPad Prism version 4.00 for Windows; GraphPad Software, San Diego, CA) and EC_{50} values were determined. Values represent the means ± S.E.M. of at least three independent experiments. The statistical significance of value differences was evaluated by the unpaired Student's t test using GraphPad Prism version 4.00 for Windows (GraphPad Software, San Diego, CA).

NMR Spectroscopy

Samples for NMR spectroscopy were prepared by dissolving the appropriate amount of A42 in a water/sodium dodecylsulfate (SDS-d_{25}) solution (pH 6.6) to obtain concentrations of 2 mM peptide and 80 mM SDS-d_{25}. Dodecyl phosphocholine samples were prepared by dissolving the appropriate amount of A42 in water/dodecyl phosphocholine (DPC-d_{38}) (pH 5.8) to obtain concentrations of 2 mM peptide and 15 mM DPC-d_{38}. NMR spectra were recorded on a Bruker DRX-600 spectrometer. One-dimensional (1D) NMR spectra were recorded in the Fourier mode with quadrature

Molecular Pharmacology Fast Forward. Published on December 6, 2005 as DOI: 10.1124/mol.105.017715
This article has not been copyedited and formatted. The final version may differ from this version.

detection and the water signal was suppressed by a low-power selective irradiation in the homogated mode. DQF-COSY, (Piantini et al., 1982), TOCSY (Braunschweiler and Ernst, 1983; Bax and Davis, 1985) and NOESY (Macura and Ernst, 1980; Jeener et al., 1979) experiments were run in the phase-sensitive mode using quadrature detection in ω_1 by time-proportional phase increment of the initial pulse (Marion and Wühtrich, 1983).

Data block sizes comprised 2048 addresses in t_2 and 512 equidistant t_1 values. Before Fourier transformation, the time domain data matrices were multiplied by shifted $\sin^2$ functions in both dimensions. A mixing time of 70 ms was used for TOCSY experiments. NOESY experiments were run at 300 K with mixing times in the range of 100-250 ms. The qualitative and quantitative analysis of DQF-COSY, TOCSY and NOESY spectra were obtained using the SPARKY interactive program package (Goddard, T. D., SPARKY 3).

Spin-Label Experiments

NMR samples were prepared by dissolving A42 at a final concentration of 2 mM in 80 mM SDS solution dissolved in H_2O/D_2O. Assuming an SDS micelle aggregation number of 56 this corresponds to a micelle concentration of 1.8 mM. The H_2O/D_2O ratio was 90/10 (Lauterwein et al., 1979). The 5- and 16-doxyl stearic acids were solubilized in methanol-d_4 and then added to the samples.

Structure Calculation

Peak volumes were translated into upper distance bounds with the routine CALIBA of the DYANA software (Guntert et al., 1997). The necessary pseudoatom corrections

Molecular Pharmacology Fast Forward. Published on December 6, 2005 as DOI: 10.1124/mol.105.017715
This article has not been copyedited and formatted. The final version may differ from this version.

were applied for non-stereospecifically assigned protons at pro-chiral centers and for the methyl group. After discarding redundant and duplicated constraints, the final list included 411 intra-residue and 125 inter-residue constraints, which were used to generate an ensemble of 200 structures by the standard protocol of simulated annealing in torsion angle space implemented in DYANA. No dihedral angle restraints and no hydrogen bond restraints were applied. The best 50 structures, which showed low values of the target functions (0.83-1.19) and small residual violations (maximum violation = 1.38 Å), were refined by *in vacuo* minimization using Discover module of MSI InsightII 2000 software, using cvff force field and applying a dielectric constant value of 1*r (MSI Molecular Symulations). The 50 structures were relaxed, firstly, constrained and then unconstrained by using a combination of steepest descent and conjugate gradients minimization algorithms until the maximum RMS derivative was less than 0.01 kcal/Å. The resulting structures showed a RMSD value of 0.9 Å on C atoms.

The minimum energy structure was subjected to a molecular dynamics procedure on peptide side chains, keeping the backbone geometry fixed. After an equilibration period of 10 ps, during which temperature was gradually increased from 10 K to 300 K, molecular dynamic simulations were run at 300 K for 600 ps. During molecular dynamics frame structures were saved each 10 fs. The final structures were analyzed using the Insight II 2000 program. (MSI Molecular Symulations). Computations were performed on a SGI Octane computer.

Molecular Pharmacology Fast Forward. Published on December 6, 2005 as DOI: 10.1124/mol.105.017715
This article has not been copyedited and formatted. The final version may differ from this version.

RESULTS

In a previous paper we have reported that the α-helical conformation of $G\alpha_s$ C-terminus is important to determine its ability to interact with the A_{2A} adenosine receptor but this part of the $G\alpha_s$ molecule is not able to stabilize the high-affinity state of the receptor (Mazzoni et al., 2000; D'Ursi et al., 2002). Moreover, we have shown that a $G\alpha_s$ C-terminal 21-residue peptide, $G\alpha_s(374\text{-}394)C^{379}A$, disrupts signal transduction and induces a conformational change of the receptor with stabilization of an intermediate affinity state for agonist ligands (Mazzoni et al., 2000). Now, we have designed and synthesized a 37 residue membrane-permeable peptide, A42, containing a 16 residue fragment (A40) derived from the homeodomain of the *Drosophila* transcription factor Antennapedia on the N-terminal side and $G\alpha_s(374\text{-}394)C^{379}A$ on the C-terminal side. A preliminary screening of cell-permeable peptide influence on PC12 cell demonstrated that pre-incubation of cell cultures with either 300 μM A40 or A42 peptide did not cause cell lysis (data not shown). The membrane-permeable $G\alpha_s$ peptide did not induce any reduction of cell viability as shown by no variation of color development after addition of the CellTiter 96® reagent between control (Abs at 490 nm, 0.24 ± 0.02; n = 4) and peptide treated (Abs at 490 nm, 0.26 ± 0.01; n = 4) cells. The effects of A40 and A42 peptides on basal and adenosine receptor (A_{2A} and A_{2B} adenosine receptors) stimulated cAMP accumulation in intact PC12 cells were evaluated. The addition of either one of the peptides had no significant effect on basal cAMP production (data not shown).

Molecular Pharmacology Fast Forward. Published on December 6, 2005 as DOI: 10.1124/mol.105.017715
This article has not been copyedited and formatted. The final version may differ from this version.

Analysis of A40 and A42 Effects on NECA-Stimulated cAMP Production in PC12 Cells.

The effects of various concentrations of A40 or A42 on cAMP accumulation induced by stimulation with 1 μM NECA were measured in PC12 cells. The membrane-permeable $G\alpha_s$ peptide inhibited adenosine receptor-mediated cAMP production in a concentration-dependent manner while the Antennapedia fragment had no major effect (Fig. 1). Analysis of data using a non-linear curve-fitting program and statistical comparison of possible fits revealed that the A42 curve was better represented by a sigmoidal dose-response curve with variable slope than a simple sigmoidal dose-response curve ($p < 0.05$). The receptor-mediated cAMP production was completely inhibited at an A42 concentration of 560 μM while the derived EC_{50} value was 5.30 ± 1.20 μM (n = 4).

To further characterize the mechanism sustaining A42 pharmacological activity, the effect of three different concentrations of the peptide on cAMP accumulation induced by PC12 stimulation with different concentrations of NECA was examined. Data obtained stimulating cells with NECA in the absence of the peptide were analyzed and fitted using a non-linear curve-fitting program (Fig. 2). Analysis revealed that the concentration-response curve was represented by a simple sigmoidal dose-response curve. The calculated EC_{50} value was 63.51 ± 10.50 nM (n = 5) whereas the maximal cAMP production was 296.81 ± 13.79 pmoles/ml. Addition of 10, 50 or 100 μM A42 caused significant reductions of NECA efficacy (Fig. 2). In fact, at a NECA concentration of 1 μM, 10 and 50 μM A42 reduced agonist efficacy by 59 and 69%, respectively, as

Molecular Pharmacology Fast Forward. Published on December 6, 2005 as DOI: 10.1124/mol.105.017715
This article has not been copyedited and formatted. The final version may differ from this version.

compared to control values in the absence of A42 (Fig. 2). The concentration-response curves obtained in the presence of 10, 50 and 100 μM A42 were fitted by a simple sigmoidal dose-response model with EC_{50} values of 84.86 ± 29.60 (n = 3), 126.10 ± 28.20 (n = 4) and 104.90 ± 24.50 (n = 3) nM, respectively, indicating that the membrane-permeable $G\alpha_s$ peptide modulated agonist potency.

Analysis of A42 specificity for disrupting G_s coupled receptors signaling

In order to verify the specificity of the A42 effect at the interface between adenosine receptors and G_s, we examined whether the membrane-permeable $G\alpha_s$ peptide was able to directly inhibit adenylyl cyclase and/or disrupt P2y12 and P2y2 receptors coupling to G_i and G_q proteins, respectively. Both subtypes of P2y receptors are expressed in PC12 cells (Unterberger et al., 2002) and it is well established that P2y12 activation leads to inhibition of adenylyl cyclase while P2y2 activation induces an increase of $[Ca^{2+}]_i$ (Ralevic and Burnstock, 1998). The A42 peptide did not influence forskolin-induced cAMP in intact PC12 cells (Fig. 3) indicating that had no direct inhibitory effect on adenylyl cyclase. In addition, the peptide did not affect P2y12 receptor mediated inhibition of cAMP production (Fig. 3). Stimulation of P2y2 receptors with 100 μM ATPγS induced a 2-fold increase of $[Ca^{2+}]_i$ in PC12 (Fig. 4) which was not modulated by the addition of A42. These results indicate that the membrane-permeable $G\alpha_s$ peptide did not influence the interactions between P2y receptors and G_i/G_q proteins supporting the specificity of peptide activity.

The ability of A42 to inhibit receptor-mediated cAMP production was also evaluated in HMEC-1, a human microvascular endothelial cell line, which constitutively expresses

Molecular Pharmacology Fast Forward. Published on December 6, 2005 as DOI: 10.1124/mol.105.017715
This article has not been copyedited and formatted. The final version may differ from this version.

both A_{2A} and A_{2B} adenosine receptors (Feoktistov et al., 2002) and β-adrenergic receptors (Gornikiewicz et al., 2000). In this cell line, A_{2B}/A_{2A} mRNA ratio is approximately 4 to 1 (Feoktistov et al., 2002) while in PC12 cells although both A_{2A} and A_{2B} mRNA were expressed (Arslan et al., 1999) the A_{2A} adenosine receptor seems to be the major adenosine receptor subtype involved in NECA stimulated effector activation in some cellular clones (Arslan et al., 1999). Indeed, HMEC-1 stimulation with 5 μM NECA induced a cAMP production of 102.07 ± 12.44 pmoles/ml while in PC12 cells stimulation with the same concentration of NECA caused a cAMP production of 296.80 ± 13.79 pmoles/ml. The A42 peptide significantly inhibited NECA stimulated cAMP production in HMEC-1 while the control peptide (A40) had no major inhibitory effect (Fig. 5). In addition, A42 inhibited β-adrenergic receptor mediated cAMP production although 1μM isoproterenol caused a moderate accumulation of cAMP (51.63 ± 10.84 pmoles/ml) in HMEC-1.

Analysis of Fluorescent A42 Peptide Internalization

To verify the ability of the A42 peptide to cross cell membranes, we synthesized a carboxy-fluorescein labeled derivative of such peptide and incubated neuronal differentiated PC12 cells in the presence and absence of a fixed concentration of such fluorescent peptide for various times. Neuronal differentiated PC12 cells were preferred over undifferentiated cells since the distribution of the fluorescent membrane-permeable peptide along the neurites can be analyzed. Living cells were labeled with the fluorescent peptide followed by membrane staining with the Image-iT™Live Plasma Membrane and Nuclear Labeling Kit. In Fig. 6, digital imagines of fluorescent cells are shown. Panels

Molecular Pharmacology Fast Forward. Published on December 6, 2005 as DOI: 10.1124/mol.105.017715
This article has not been copyedited and formatted. The final version may differ from this version.

A and B of Fig. 6 illustrate cell labeling with the fluorescein conjugated A42 peptide (green-fluorescence) after 30 min and 3 h of incubation, respectively. At 30 min, the fluorescent peptide was localized on plasma membrane in both cell bodies and neurites while after 3 and 6 h (data not shown) the fluorescent staining was detectable inside cells. The fluorescein (green-fluorescence) staining overlapped the Alexa Fluor 594 wheat germ agglutinin (red-fluorescence) staining on plasma membranes (Fig. 6, panel C and D).

NMR Spectroscopy.

The membrane environment for NMR studies is usually mimicked by surfactant supra-molecular aggregates generally constituted by an apolar inner core and a hydrophilic exposed interface. Although a variety of surfactant supra-molecular structures have been proposed for NMR analysis, the choice is limited due to the high costs of the surfactant deuteration and usually low quality of spectra produced in such systems. Micellar solutions of SDS, DPC and dipalmitoyl phosphatidyl cholin (DPPC) are typically used for NMR investigations (Bader et al., 2003).

A whole set of 1D and 2D protonic spectra were recorded in aqueous solution of 80 mM SDS and 15 mM DPC solution. To check the absence of peptide aggregation states, spectra were acquired within the concentration range of 0.5-15 mM. No significant changes were observed in the distribution and shape of the ^{1}H resonances indicating that no aggregation phenomena occurred within this concentration range.

Due to the better quality of SDS NMR spectra vs DPC NMR spectra, the complete resonance assignments of A42 were achieved in SDS micellar solution according to the

Molecular Pharmacology Fast Forward. Published on December 6, 2005 as DOI: 10.1124/mol.105.017715
This article has not been copyedited and formatted. The final version may differ from this version.

method of Wüthrich (Wüthrich, 1986) *via* the usual systematic application of DQF-COSY (Piantini et al., 1982), TOCSY (Braunschweiler and Ernst, 1983; Bax and Davis, 1985) and NOESY (Macura and Ernst 1980; Jeener et al., 1979) experiments with the support of SPARKY software package (Goddard, T. D., SPARKY 3). The resonances of several CHα were up-field shifted, suggesting the involvement of these residues in α-helix or in turn secondary structure (Wishart et al., 1991).

The pattern of NOE connectivities observed in NOESY spectra (data not shown) were consistent with the presence of two helical stretches localized at N- and C-termini of the A42 peptide. In Fig. 7 and 8, the N- and C-terminal helices are represented with cyan and violet ribbons, respectively. Low regularity in the dihedral angle patterns was detectable at the level of residues 11-17.

Structure Calculation.

Three-dimensional structures of A42 were calculated by simulated annealing in torsion angle space and restrained molecular dynamics methods based on 536 NOE-derived restraints, using DYANA software package (Guntert et al., 1997). Among 200 calculated structures, the resulting best 50 ones were selected according to the lowest values of their target function. They were subjected to further procedures of minimization by Discover module of Insight II [MSI] (MSI Molecular Symulations) using the DYANA derived restraints with a force constant value = 1. The inspection of the torsion angles according to the PROCHECK (Laskowski et al., 1996) software pointed out, for the most of the calculated structures, the presence of two separate helical

Molecular Pharmacology Fast Forward. Published on December 6, 2005 as DOI: 10.1124/mol.105.017715
This article has not been copyedited and formatted. The final version may differ from this version.

regions including residues 3-10 and 18-35. In Table 1 the statistic of the structure calculation is reported.

Spin-Label Studies.

The positioning of the peptide relative to the surface and interior of the SDS micelle was studied using the following paramagnetic probes: 5- and 16-doxyl stearic acids. Both compounds contain doxyl headgroups, a cyclic nitroxide with unpaired electron, which is bound to the aliphatic chain carbon in position 5 or 16, respectively. These paramagnetic probes are expected to cause broadening of the NMR signals and decrease of resonance intensities from residues inside but close to the surface (5-doxyl), or deeply buried in the micelle (16-doxyl), respectively (Jarvet et al., 1997; Lindberg et al., 2001).

TOCSY spectra of A42 in the presence and absence of the spin labels were recorded keeping constant all other conditions. Just few residues were affected by the presence of 5-doxylstearic acid. Particularly, Asp^{21} and Met^{29} NH/α signals nearly disappeared. On the other hand, the A42 spectrum, acquired in the presence of 16-doxyl stearic acid, evidenced that Arg^{1}, Gln^{2}, Ile^{3}, Phe^{7}, Arg^{11}, Lys^{13}, Lys^{15}, Val^{18}, Phe^{19}, Ala^{22}, Arg^{23}, Ile^{25}, Met^{29}, Leu^{36}, Leu^{37} were drastically affected by 16-doxylstearic acid with a nearly disappearing of NH/α signals. These results provided strong evidences that A42 had a significant preference to be deeply buried in the micelles.

Molecular Pharmacology Fast Forward. Published on December 6, 2005 as DOI: 10.1124/mol.105.017715
This article has not been copyedited and formatted. The final version may differ from this version.

DISCUSSION

The increasing knowledge of disease molecular basis has prompted the development of new classes of specific drugs such as peptide/polypeptide- or DNA-based drugs. Unfortunately often these bio-molecules show limited ability to cross plasma membrane resulting in poor cellular access which largely prohibits them from reaching intracellular targets.

We previously developed a $G\alpha_s$ 21 residue synthetic peptide that inhibits A_{2A} adenosine receptor-mediated activation of adenylyl cyclase in rat striatal membranes (Mazzoni et al., 2000). Here, we created a cell-permeating version of such peptide by N-terminal modification with the cell permeation sequence (16 residues) from the homeodomain of Antennapedia. Besides studying the biological activity and intracellular transfer of the cell-permeable $G\alpha_s$ peptide, its structural properties were analyzed by NMR. This part of the work was a necessary step to confirm the ability of the $G\alpha_s$ segment to acquire an α-helical conformation ((Mazzoni et al., 2000) even in the contest of a chimeric peptide. The α-helix structure of the 21-residue $G\alpha_s$ peptide overlaps that of $G\alpha_s$ C-terminus shown by the crystal structure resolution (Sunahara et al., 1997) and is pivotal for its biological activity (Mazzoni et al., 2000). In addition, structural studies of the chimeric peptide in a membrane mimicking environment are useful to elucidate the mechanism of penetratin internalization, an issue which is still debated (Richard et al., 2003).

The Membrane-Permeable $G\alpha_s$ Peptide Is an Inhibitor of Receptor-Stimulated cAMP Production in PC12 Cells and HMEC-1.

Molecular Pharmacology Fast Forward. Published on December 6, 2005 as DOI: 10.1124/mol.105.017715
This article has not been copyedited and formatted. The final version may differ from this version.

The membrane-permeable $G\alpha_s$ peptide (A42) did not affect cell viability but significantly inhibited adenosine receptor-mediated cAMP accumulation in PC12 cells while the permeation sequence (A40) did not show any effect. These results prompted us to investigate the pharmacological profile of this inhibition by studying the concentration-dependent effect of the peptide. The A42 peptide was a potent inhibitor of cAMP accumulation in PC12 cells with an EC_{50} value of approximately 5 μM. The membrane-permeable peptide caused a dramatic decrease of agonist maximal efficacy. This effect was evident at a peptide concentration close to its EC_{50} value. At higher peptide concentrations NECA potency was also modulated. The observed reduction of NECA efficacy suggests that A42 compete with $G\alpha_s$ for interaction with adenosine receptor leading to a decreased number of activated $G\alpha_s$. The molecular basis supporting the decrease of NECA potency are less evident but a shift of receptor affinity state for agonist ligands may be involved as suggested by our previous observations (Mazzoni et al., 2000). In contrast to direct Gα protein inhibitors such as suramin and analogues (Freissmuth et al., 1999) the inhibition caused by A42 appears to be mixed competitive. Whereas suramin acts with several mechanisms in preventing receptor mediated G protein activation including suppression of spontaneous GDP-release from Gα subunits and competition with receptors for binding to G proteins (Freissmuth et al., 1999) our membrane-permeable $G\alpha_s$ peptide does not directly modulate GDP/GTP exchange but it competes with $G\alpha_s$ for interacting with receptors. Thus, A42 decreasing the number of productive receptor G_s interactions causes reduction of agonist efficacy while its binding to the receptor induces a decrease of receptor affinity for the agonist which appears as

Molecular Pharmacology Fast Forward. Published on December 6, 2005 as DOI: 10.1124/mol.105.017715
This article has not been copyedited and formatted. The final version may differ from this version.

reduction of agonist potency.

The 42 peptide did not directly modulate adenylyl cyclase activity and did not affect G_i and G_q coupled receptor signaling. Such observations are indicative that the specific peptide target is the receptor G_s interface. Sequence alignment of $G\alpha_s$, $G\alpha_i$ and $G\alpha_q$ C-termini shows that the differences are restricted to few key regions. However, these key residues are the structural determinants of receptor $G\alpha$ specificity of interaction (Cabrera-Vera et al., 2003). Our 21 residue $G\alpha_s$ peptide was chosen on the basis of its ability to inhibit A_{2A} adenosine receptor mediated production of cAMP in rat striatal membranes (Mazzoni et al., 2000) while an eleven residue peptide was less effective. However, we must point out that since the A_{2A} adenosine receptor in rat striatum is coupled to G_{olf} (Corvol et al., 2001) we may have directed our selection toward a tool effective in disrupting their interaction. On the other hand, G_{olf} shares extensive amino acid identity with $G\alpha_s$ (Jones and Reed, 1989) and divergences are not localized in the extreme C-terminal region. Others (Feldman et al., 2002) have shown that an 83 residue polypeptide derived from the C-terminus of $G\alpha_s$ specifically inhibits G_s signaling in HEK-293 cells. The A42 peptide was able to inhibit adenosine and β-adrenergic receptor mediated cAMP production in a human cell line (HMEC-1) although with a lower effectiveness than in PC12 cells. This observation may indicate a certain selectivity of the peptide for inhibiting A_{2A} adenosine receptor coupling to G_s proteins or may result as a consequence of the different ability of A42 to penetrate human endothelial cell plasma membrane.

The use of the carboxy-fluorescein labeled A42 peptide proved to be a very effective

Molecular Pharmacology Fast Forward. Published on December 6, 2005 as DOI: 10.1124/mol.105.017715
This article has not been copyedited and formatted. The final version may differ from this version.

strategy to verify peptide translocation inside differentiated PC12 cells. Within 30 min the A42 peptide is localized exclusively on plasma membrane while later (3-6 h) is distributed between plasma membrane and cytoplasm. These results are particularly relevant since they are obtained in live cells and correlate the peptide localization on plasma membrane with its ability to inhibit adenosine receptor mediated activation of the G_s protein.

The employment of membrane-permeable peptides to disrupt protein/protein interfaces and thus manipulate intracellular signaling pathways has attracted the interest of numerous investigators. Various peptides (cargo) have been successfully delivered inside cells through their conjugation to cell penetrating peptides (carrier) such as pentratin(43-58) and transactivating regulatory protein (TAT)(49-57) (Eiden, 2005).

Two types of approaches have been used in the past to inhibit signaling from G_s-coupled receptors in intact cells. Chang et al. (2000) have successfully created a membrane-permeable $G\alpha_s$ peptide by fusing with a chemical reaction the Kaposi fibroblast growth factor signal sequence (MPS) to the N-terminus of $G\alpha_s$ last 11 residue fragment. On the other hand, Feldman et al. (2002) have selectively inhibited G_s signaling in HEK-293 cells by transfection with a minigene encoding for a 83 residue polypeptide derived from the C-terminus of $G\alpha_s$. Both approaches have produced interesting and useful results but also present some inconveniences which need improvements. In the case of the MPS-fused peptide the $G\alpha_s$ C-terminal sequence is rather short and the membrane-permeable peptide is obtained using chemical oxidation followed by conjugation. The whole A42 peptide was synthesized by the conventional

Molecular Pharmacology Fast Forward. Published on December 6, 2005 as DOI: 10.1124/mol.105.017715
This article has not been copyedited and formatted. The final version may differ from this version.

solid-phase strategy. On the other hand the minigene approach cannot be suitable for all cell types.

NMR Analysis Reveals the α-Helical Conformation and Preference for a Hydrophobic Environment of the Membrane-Permeable Gα$_s$ Peptide.

Structural data can support the interpretation of biological observations in the key of significant bio-molecular interactions. Accordingly, we undertook a full NMR investigation of the A42 peptide in membrane mimetic environments in order to compare its structure to that of the 21 residue Gα$_s$ peptide, previously described (Mazzoni et al., 2000). The choice of the membrane-like solvent was motivated on the fact that both the penetratin and the Gα$_s$ segments are involved in membrane interactions.

NMR spectra were record in SDS and DPC micellar solutions but data of the best quality were obtained in SDS micellar solutions. At a greater concentration than its critical micellar concentration (8 mM at 25°C) NMR experiments showed that A42 was arranged in two stretches of α-helical structure encompassing respectively residues 3-10 and 18-36. It is noticeable that even in a membrane mimicking environment and in conjugation with a cell penetrating peptide, the segment 18-36 can be well overlapped with the previous solved structure of the corresponding Gα$_s$(374-394)C^{379}A peptide (D'Ursi et al., 2002) and even with the crystal structure of the Gα$_s$ protein (Sunahara et al., 1997). This demonstrates that the presence of the penetratin segment does not affect the conformational stability and functionality of the Gα$_s$(374-394)C^{379}A peptide.

Molecular Pharmacology Fast Forward. Published on December 6, 2005 as DOI: 10.1124/mol.105.017715
This article has not been copyedited and formatted. The final version may differ from this version.

The inspection of the electrostatic surface showed that the helix 18-36 was amphipathic (Fig. 7) with the presence of a polar surface lined by Asp^{378}, Arg^{380}, Asp^{381}, and Arg^{385} and two hydrophobic surfaces defined by less polar residues Ile^{382}, Ile^{383}, Met^{386}, His^{387}, Tyr^{391}, and Leu^{393}. The analysis of the side chain assessment and the comparison with the $G\alpha_s(374\text{-}394)C^{379}A$ structure highlighted that Asp^{378}, Asp^{381}, Ile^{383} and Leu^{388} were in a significantly ordered conformation (Fig. 7A). Several studies attribute an important role to these amino acids as highly conserved residues directly involved in G protein receptor interaction (Kisselev et al., 1998). In particular, it has been demonstrated by numerous biological evidences that a constant of the GPCR/G protein coupling is an electrostatic interaction involving highly conserved Asp residues of Gα C-terminal region with the highly conserved DRY motif of the receptors (Kisselev et al., 1998). These contacts seem to be stabilized by multi-helix interaction with C-terminal residues of the receptor involving several conserved hydrophobic residues such as Ile^{383} and Leu^{388}.

It is interesting that the arrangement of the side chains of the 18-36 helix in A42, in particular of those residues retained important for the interaction with the cognate receptor (Kisselev et al., 1998), was comparable to the orientation observed in the C-terminal $G\alpha_t$ undecapeptide structure derived from the model of the G protein/receptor complex proposed by Koenig et al. (2002) (Fig. 8). Thus, a consistency was evident between the models of the C-terminal Gα helix, in the whole receptor/G protein complex and those of its related $G\alpha_s(374\text{-}394)C^{379}A$ peptide, even conjugated with a delivery molecule. There are sufficient data to believe that the conservation of these fundamental

Molecular Pharmacology Fast Forward. Published on December 6, 2005 as DOI: 10.1124/mol.105.017715
This article has not been copyedited and formatted. The final version may differ from this version.

structural characters is responsible for the activity of the C-terminal peptide as that of the whole $G\alpha_s$ protein.

TOCSY experiments of A42 in micelle solution, acquired alternatively, in the presence of 5, and 16-doxyl stearic acids, showed that the peptide was generally more sensitive to the action of 16 doxyl-stearic acid, the inner core probe of the micelle. In particular, among the residues affected by 16-doxyl-stearic acid, four residues belonged to the C-terminal penetratin portion. These data supported the structural determinant of the penetratin delivery ability and showed that the conjugation of the penetratin peptide with a cargo did not affect the modality of its delivery functionality.

The distribution of the molecular surface of the penetratin segment as compared to the $G\alpha_s(374\text{-}394)C^{379}A$ portion in A42 allows to formulate a hypothesis on how the fine arrangement of the side chains can be related to the functionality of the bio-molecule. While the distribution of polar and hydrophobic residues defined an amphipathic α-helix in the $G\alpha_s(374\text{-}394)C^{379}A$ region, which seemed tailored to allow peptide key interactions with receptors in the penetratin region the distribution of the side chains is in such way to form clusters of hydrophobic and hydrophilic surfaces at the N-terminus and in the center of the fragment, respectively (Fig. 7B). The clustering of hydrophobic and hydrophilic residues is consistent with the most recent hypotheses which reestablish the role of endocytosis in the internalization of cationic CPP (Richard et al., 2003). The effect of the spin labels induces to speculate on the A42 segment boundary that is inserted in the core of the micelle. In fact, the experiments in the presence of 5-doxyl stearic acid

Molecular Pharmacology Fast Forward. Published on December 6, 2005 as DOI: 10.1124/mol.105.017715
This article has not been copyedited and formatted. The final version may differ from this version.

showed that only few residues were localized in proximity of the micelle surface. In particular the residues 19 and 20 corresponding to the N-terminal region of the $G\alpha_s$(374-394)C^{379}A portion were those significantly sensitive to the action of the surface probe of the micelle so that in a transport process they can define the boundary between the region inserted in the membrane and that exposed on the surface.

In conclusion, our biological data in conjugation with conformational analysis and fluorescence microscopy studies point out that the A42 peptide is a valuable, non-toxic research tool to modulate G_s-coupled receptor signal transduction. These results represent the starting point for the development of new peptomimetic drug candidates acting at the intracellular level.

ACKNOWLEDGMENTS

We are grateful to A. Asta for her expert technical assistance.

REFERENCES

Arslan G, Kull B, Fredholm BB (1999) Signaling via A_{2A} adenosine receptor in four PC12 cell clones. *Naunyn Schmiedebergs Arch Pharmacol* 359: 28-32.

Bader R, Lerch M, Zerbe O (2003) NMR of membrane-associated peptides and proteins. Methods and Principles in Medicinal Chemistry. *BioNMR in Drug Research* 16: 95-120.

Bax A, Davis DG (1985) Mlev-17-based two-dimensional homonuclear magnetization transfer spectroscopy. *J Magn Reson* 65: 355-360.

Braunschweiler L, Ernst RR (1983) Coherence transfer by isotropic mixing: application to proton correlation spectroscopy. *J Magn Reson* 53: 521-528.

Cabrera-Vera TM, Vanhauwe J, Thomas TO, Medkova M, Preininger A, Mazzoni MR, Hamm HE (2003) Insights into G protein structure, function, and regulation. *Endocr Rev* 24: 765-781.

Ceccarelli F, Scavuzzo MC, Giusti L, Bigini G, Costa B, Carnicelli V, Zucchi R, Lucacchini A, Mazzoni MR (2003) ET_A receptor-mediated Ca^{2+} mobilisation in H9c2 cardiac cells. *Biochem Pharmaco*. 65: 783-793.

Chang M, Zhang L, Tam JP, Sanders-Bush E (2000) Dissecting G protein-coupled receptor signaling pathways with membrane-permeable blocking peptides. Endogenous 5-HT_{2C} receptors in choroid plexus epithelial cells. *J Biol Chem* 275: 7021-7029.

Corvol JC, Studler JM, Schonn JS, Girault JA, Herve D (2001) $G\alpha_{olf}$ is necessary for coupling D1 and A2a receptors to adenylyl cyclase in the striatum. *J Neurochem* 76: 1585-1588.

Derossi D, Joliot AH, Chassaing G, Prochiantz A (1994) The third helix of the Antennapedia homeodomain translocates through biological membranes. *J Biol Chem* 269: 10444-10450.

D'Ursi AM, Albrizio S, Greco G, Mazzeo S, Mazzoni MR, Novellino E, Rovero P (2002) Conformational analysis of the Gα protein C-terminal portion. *J Pept Sci* 8: 576-588.

Eiden LE (2005) Fusion polypeptides that inhibit exocytosis: fusing aptamer and cell-penetrating peptide technologies and pharmacologies. *Mol Pharmacol* 67: 980-982.

Feldman DS, Zamah AM, Pierce KL, Miller WE, Kelly F, Rapacciuolo A, Rockman HA, Koch WJ, Luttrell LM (2002) Selective inhibition of heterotrimeric Gs signaling. Targeting the receptor-G protein interface using a peptide minigene encoding the $G\alpha_s$ carboxyl terminus. *J Biol Chem* 277: 28631-28640.

Feoktistov I, Goldstein AE, Ryzhov S, Zeng D, Belardinelli L, Voyno-Yasenetskaya T, Biaggioni I (2002) Differential expression of adenosine receptors in human endothelial cells: role of A_{2B} receptors in angiogenic factor regulation. *Circ Res* 90: 531-538.

Freissmuth M, Waldhoer M, Bofill-Cardona E, Nanoff C (1999) G protein antagonists. Trends Pharmacol Sci 20: 237-245.

Gilchrist A, Bunemann M, Li A, Hosey MM, Hamm HE (1999) A dominant-negative strategy for studying roles of G proteins in vivo. *J Biol Chem* 274: 6610-6616.

Gornikiewicz A, Sautner T, Brostjan C, Schmierer B, Fugger R, Roth E, Muhlbacher F, Bergmann M (2000) Catecholamines up-regulate lipopolysaccharide-induced IL-6 production in human microvascular endothelial cells. *FASEB J* 14: 1093-1100.

Guntert P, Mumenthaler C, Wüthrich K (1997) Torsion angle dynamics for NMR structure calculation with the new program DYANA. *J Mol Biol* 273: 283-298.

Havlickova M, Blahos J, Brabet I, Liu J, Hruskova B, Prezeau L, Pin JP (2003) The second intracellular loop of metabotropic glutamate receptors recognizes C termini of G-protein α-subunits. *J Biol Chem* 278: 35063-35070.

Jarvet J, Zdunek J, Damberg P, Graslund A (1997) Three-dimensional structure and position of porcine motilin in sodium dodecyl sulfate micelles determined by 1H NMR. *Biochemistry* 36: 8153-8163.

Jeener J, Meyer BH, Bachman P, Ernst RR (1979) Investigation of exchange processes by two-dimensional NMR spectroscopy. *J Chem Phys* 71: 4546-4553.

Jones DT, Reed RR (1989) Golf: an olfactory neuron specific-G protein involved in odorant signal transduction. *Science* 244: 790-795.

Kisselev OG, Kao J, Ponder JW, Fann YC, Gautam N, Marshall GR (1998) Light-activated rhodopsin induces structural binding motif in G protein α-subunit. *Proc Natl Acad Sci USA* 95: 4270-4275.

Kobilka BK, Kobilka TS, Daniel K, Regan JW, Caron MG, Lefkowitz RJ (1988) Chimeric α2-, β2-adrenergic receptors: delineation of domains involved in effector coupling and ligand binding specificity. *Science* 240: 1310-1316.

Koenig BW, Kontaxis G, Mitchell DC, Louis JM, Litman BJ, Bax A (2002) Structure and orientation of a G protein fragment in the receptor bound state from residual dipolar couplings. *J Mol Biol* 322: 441-461.

Kostenis E, Conklin BR, Wess J (1997) Molecular basis of receptor/G protein coupling selectivity studied by coexpression of wild type and mutant m_2 muscarinic receptors with mutant $G\alpha_q$ subunits. *Biochemistry* 36: 1487-1495.

Laskowski RA, Rullmannn JA, MacArthur MW, Kaptein R, Thornton JM (1996) AQUA and PROCHECK-NMR: programs for checking the quality of protein structures solved by NMR. *J Biomo NMR* 8: 477-486.

Lauterwein J, Bosch C, Brown LR, Wüthrich K (1979) Physiochemical studies of the protein-lipid interactions in melittin containing micelles. *Biochim Biophys Acta* 556: 244-264.

Lindberg M, Jarvet J, Langel U, Graslund A (2001) Secondary structure and position of the cell-penetrating peptide transportan in SDS micelles as determined by NMR. *Biochemistry* 40: 3141-3149.

Macura S, Ernst RR (1980) Elucidation of cross relaxation in liquids by two-dimensional NMR spectroscopy. *Mol Phys* 41: 95-117.

Marion D, Wühtrich K (1983) Application of phase sensitive two-dimensional correlated spectroscopy (COSY) for measurements of ^{1}H-^{1}H spin-spin coupling constants in proteins. *Biochem Biophys Res Commun* 113: 967-974.

Mazzoni MR, Taddei S, Giusti L, Rovero P, Galoppini C, D'Ursi A, Albrizio S, Triolo A, Novellino E, Greco G, Lucacchini A, Hamm HE (2000) A $G\alpha_s$ carboxyl-terminal peptide prevents G_s activation by the A_{2A} adenosine receptor. *Mol Pharmacol* 58: 226-236.

Piantini U, Soerensen OW, Ernst RR (1982) Multiple quantum filters for elucidating NMR coupling networks. *J Am Chem Soc* 104: 6800-6801.

Ralevic V, Burnstock G (1998) Receptors for purines and pyrimidines. *Pharmacol Rev* 50: 413-492.

Richard JP, Melikov K, Vives E, Ramos C, Verbeure B, Gait MJ, Chernomordik LV, Lebleu B. (2003) Cell-penetrating peptides. A reevaluation of the mechanism of cellular uptake. J *Biol Chem* 278: 585-590.

Slessareva JE, Ma H, Depree KM, Flood LA, Bae H, Cabrera-Vera TM, Hamm HE, Graber SG (2003) Closely related G-protein-coupled receptors use multiple and distinct domains on G-protein α-subunits for selective coupling. *J Biol Chem* 278: 50530-50536.

Sunahara RK, Tesmer JJ, Gilman AG, Sprang SR (1997) Crystal structure of the adenylyl cyclase activator $G\alpha_s$. *Science* 278: 1943-1947.

Unterberger U, Moskvina E, Scholze T, Freissmuth M, Boehm S (2002) Inhibition of adenylyl cyclase by neuronal P2Y receptors. *Br J Pharmacol* 135: 673-684.

Vanhauwe JF, Thomas TO, Minshall RD, Tiruppathi C, Li A, Gilchrist A, Yoon EJ, Malik AB, Hamm HE (2002) Thrombin receptors activate G_o proteins in endothelial cells to regulate intracellular calcium and cell shape changes. *J Biol Chem* 277: 34143-34149.

Wishart DS, Sykes BD, Richards FM (1991) Relationship between Nuclear Magnetic Resonance chemical shift and protein secondary structure. *J Mol Biol* 222: 311-333.

Wüthrich K (1986) NMR of proteins and nucleic acids. John Wiley & Sons, Inc., New York, NY.

Molecular Pharmacology Fast Forward. Published on December 6, 2005 as DOI: 10.1124/mol.105.017715
This article has not been copyedited and formatted. The final version may differ from this version.

FOOTNOTES

a) This work was supported by Ministero dell'Istruzione, dell'Universitá e della Ricerca (MIUR) grants to A. Lucacchini and M.R. Mazzoni and by a grant from Fondazione Ente Cassa di Risparmio di Firenze to P. Rovero.

b) Maria R. Mazzoni, Dipartimento di Psichiatria, Neurobiologia, Farmacologia e Biotecnologie - Sezione di Neurobiologia e Famacologia - Via Bonanno 6, 56126, Pisa, Italy; Tel., +39-050-2219524; Fax, +39-050-2219609; e-mail, mariarm@farm.unipi.it.

c) [1]A.M. D'Ursi and L. Giusti contributed equally to the work.

Molecular Pharmacology Fast Forward. Published on December 6, 2005 as DOI: 10.1124/mol.105.017715
This article has not been copyedited and formatted. The final version may differ from this version.

LEGENDS FOR FIGURES

Fig. 1. Concentration-dependent effect of A40 and A42 peptides on NECA-stimulated cAMP production in PC12 cells. PC12 cells were incubated with various concentrations of either A40 or A42 in the presence of 1 μM NECA as described in *Materials and Methods*. Control value in the absence of peptides was 304.12 ± 15.09 pmoles cAMP/ml (n = 5). Values are the mean ± S.E.M. of three (A40) and five (A42) independent experiments each performed in duplicate. The EC_{50} value was determined by fitting data as a sigmoidal dose-response curve with variable slope using the GraphPad Prism version 4.00 computer program.

Fig. 2. Modulation of NECA-stimulated cAMP production by the A42 peptide in PC12 cells. PC12 cells were incubated with different concentrations of NECA in the presence and absence of 10, 50 or 100 μM A42. Accumulation of cAMP was determined as described in *Materials and Methods*. In the absence of both NECA and A42, basal value of cAMP accumulation was 1.10 ± 0.40 pmoles/ml (n = 5) whereas in the presence of 10, 50 and 100 μM A42 basal values were 0.70 ± 0.14 (n = 3), 1.02 ± 0.22 (n = 4) and 1.41 ± 0.10 (n = 3) pmoles/ml. Values are the mean ± S.E.M. of three to five independent experiments each performed in duplicate. The EC_{50} values were determined by fitting data as sigmoidal dose-response curves using the GraphPad Prism version 4.00 computer program.

Molecular Pharmacology Fast Forward. Published on December 6, 2005 as DOI: 10.1124/mol.105.017715
This article has not been copyedited and formatted. The final version may differ from this version.

Fig. 3. The A42 peptide does not directly modulate adenylyl cyclase and $P2y_{12}$ receptor signaling to G_i. PC12 cells were preincubated in the presence and absence of 10 μM forskolin with and without 100 μM A42 for 30 min at 37ºC. Then, some samples were stimulated with 1 μM ADPβS. Accumulation of cAMP was determined as described in *Materials and Methods*. Values are the mean ± S.E.M. of three independent experiments each performed in duplicate. Values that are significantly different from either basal (*, $p < 0.05$) or forskolin stimulated ($^{\#}$, $p < 0.05$) value as determined by unpaired Student's t test are indicated.

Fig. 4. The A42 peptide does not affect $P2y_2$-mediated increase of $[Ca^{2+}]_i$ in PC12 cells. Confluent PC12 cells cultured in 24 well plates were incubated with and without 100 μM A42 in a loading buffer containing 2 μM Fluo-3 AM and 0.008% Pluronic F-127 for 30 min at 37°C. Cells were detached, harvested and analysed on a FACScan flow cytometer as described in Materials and Methods. The basal fluorescence was recorded for each sample and then the agonist (100 μM ATPγS) was added. The basal $[Ca^{2+}]_i$ was determined as described (Ceccarelli et al., 2003). Values are the mean ± S.E.M. of three independent experiments each performed in duplicate.

Fig. 5. Inhibition of NECA- and isoproterenol-stimulated cAMP production by the A42 peptide in HMEC-1. Confluent HMEC-1 cultured in 24 well plates were incubated with and without 100 μM A42 in complete MCDB 131 medium containing 100 μM papaverine for 30 min at 37ºC. Then, either 5 μM NECA or 1 μM isoproterenol was

Molecular Pharmacology Fast Forward. Published on December 6, 2005 as DOI: 10.1124/mol.105.017715
This article has not been copyedited and formatted. The final version may differ from this version.

added to appropriate wells. Accumulation of cAMP was determined as described in *Materials and Methods*. Values are the mean ± S.E.M. of three independent experiments each performed in duplicate. Value that are significantly different from control value (**, $p < 0.01$) as determined by unpaired Student's t test are indicated.

Fig. 6. Fluorescence photomicrographs of neuronal differentiated PC12 live-cells. In A and C cells were incubated with the fluorescent peptide for 30 min whereas in B and D for 3h. In C and D cells were stained with Image-iT LIVE Kit labelling plasma membranes with Alexa Fluor 594 wheat germ agglutinin (red-fluorescent). Scale bar: 20 μm.

Fig. 7. NMR structure of A42 in SDS micellar solution (600Mhz, 300K, mixing time 150 ms). The helical stretches are outlined by cyan (penetratin) and violet ($G\alpha_s$) ribbons. The electrostatic surfaces of 18-36 (A) and 3-10 α-helices (B) are displayed. A: Electrostatic surface of 18-36 region of A42. Polar region (colored in blue) is lined by residues corresponding to Asp^{21}, Arg^{23}, Asp^{24}, and Arg^{28}. Two hydrophobic planes (colored in red) are defined by less polar residues Ile^{25}, Ile^{26}, Met^{29}, His^{30}, Tyr^{34}, and Leu^{36}. B: Electrostatic surface of 3-10 α-helical fragment. The side chains defining clusters of hydrophobic (Trp) and hydrophilic residues are displayed and colored according to their hydrophobicity.

Molecular Pharmacology Fast Forward. Published on December 6, 2005 as DOI: 10.1124/mol.105.017715
This article has not been copyedited and formatted. The final version may differ from this version.

Fig. 8. Comparison of the conformational properties of the last 11 C-terminal residues of A42 (NMR structure in micellar solution) (blue) and the corresponding region of $G\alpha_t$ derived from Koenig's model (orange) (Koenig et al, 2002). The side chains of fragments are displayed and colored according to their hydrophobicity.

Molecular Pharmacology Fast Forward. Published on December 6, 2005 as DOI: 10.1124/mol.105.017715
This article has not been copyedited and formatted. The final version may differ from this version.

Table 1. Statistical information for A42 structure calculation.

Distant restraints	Total	536
	Intra-monomer	411
	Inter-monomer	125
	Sequential (i-j = 1)	78
	Medium (i-j = 2, 3, 4)	47
RMSD analysis	Ile^{3}-Arg^{10} backbone	0.83 ± 0.30 Å
	Ile^{3}-Arg^{10} heavy atoms	1.75 ± 0.43 Å
	Asn^{20}-Tyr^{34} backbone	0.96 ± 0.48 Å
	Asn^{20}-Tyr^{34} heavy atoms	1.85 ± 0.60 Å
NOEs violations >0.1 Å	Total violations	7
	Highest	0.27
	Lowest	0.12
	Average violation (Å)	0.17 ± 0.05
Average energy (Kcal/mol)	Total energy	600 ± 5
	Bond energy	120 ± 1
	Phi energy	28 ± 3
	Theta energy	235 ± 7
	Out of plane energy	0.91 ± 0.03
	Non-bonded energy	217 ± 12

Fig. 1

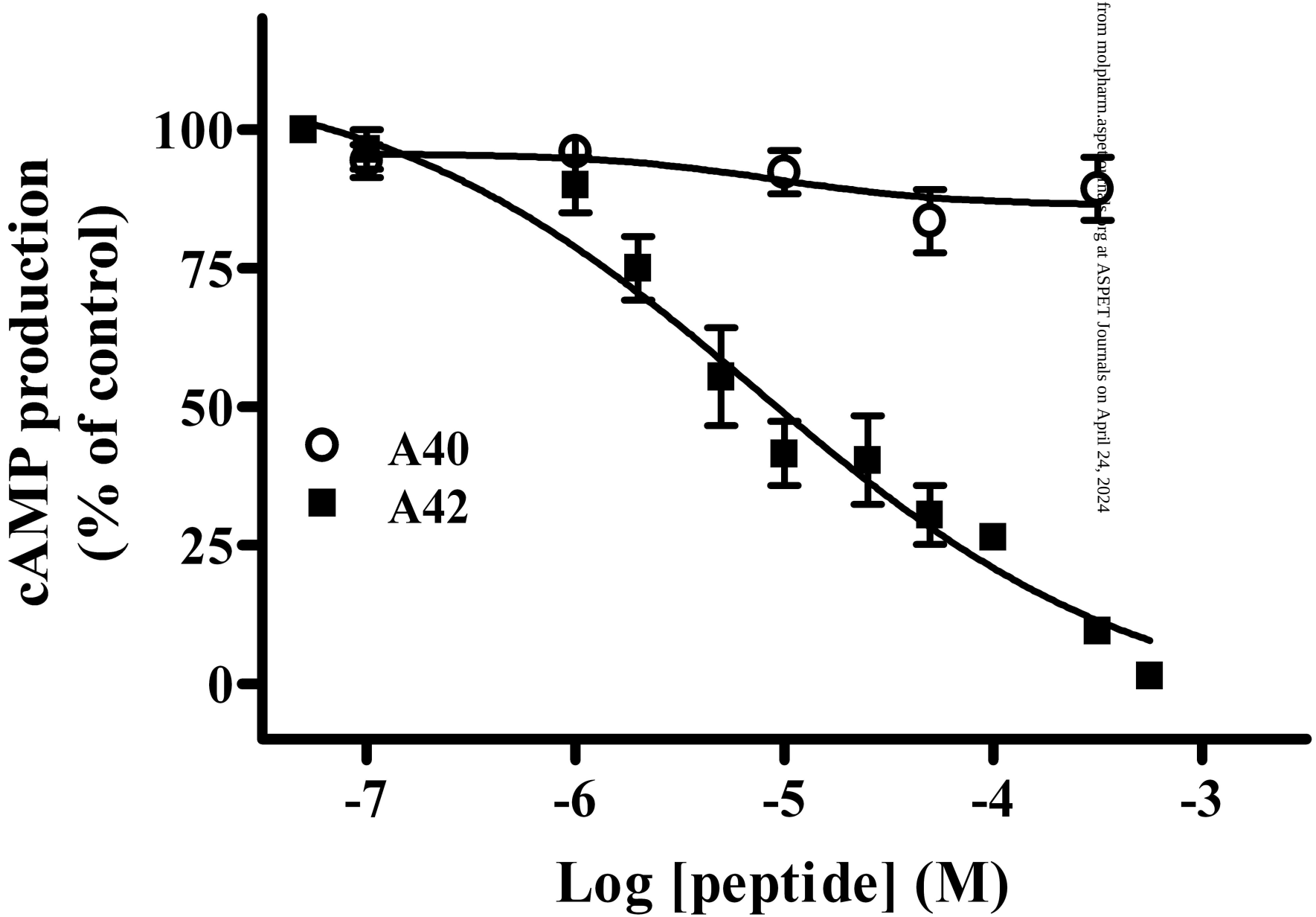

Fig. 2

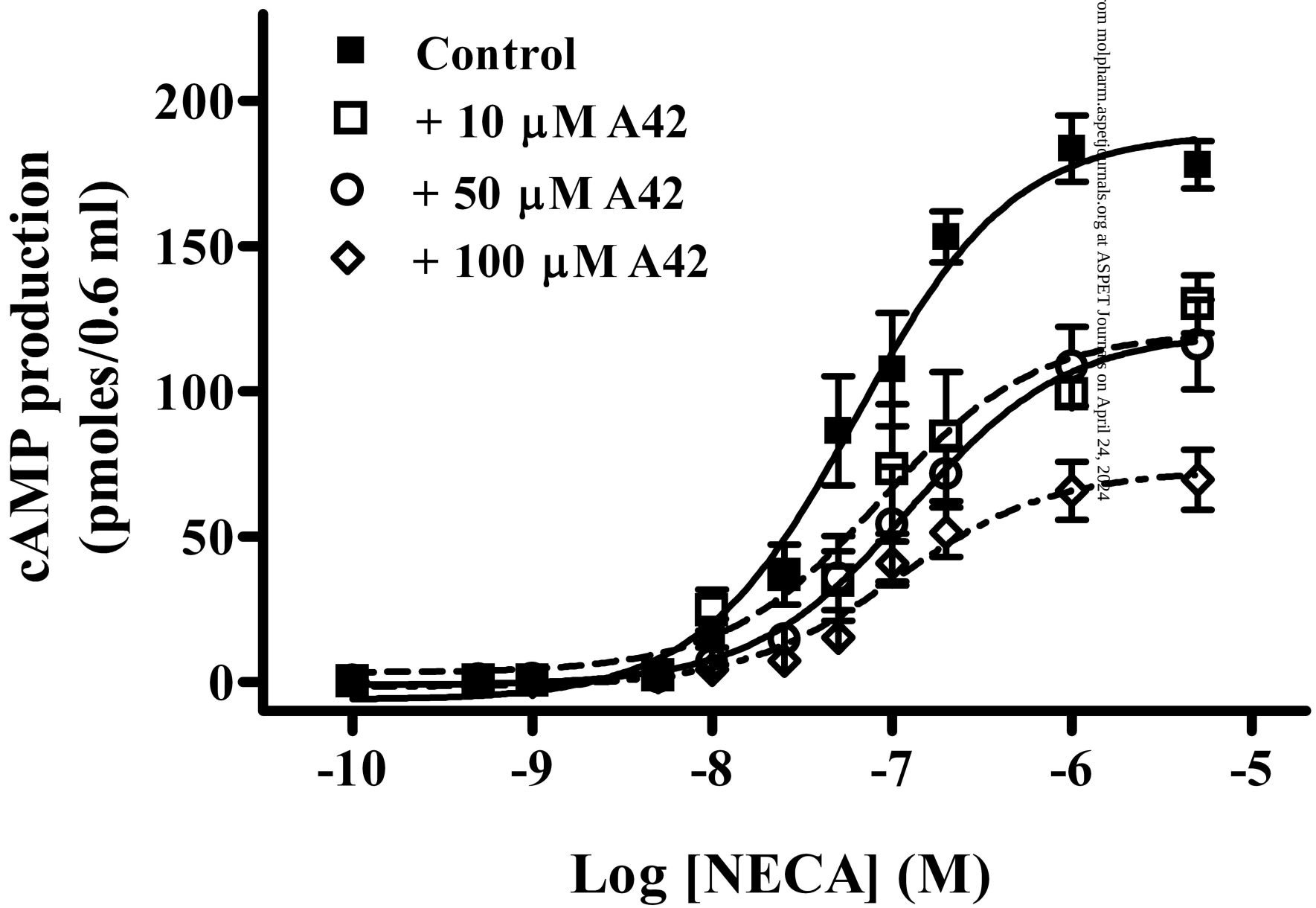

Fig. 3

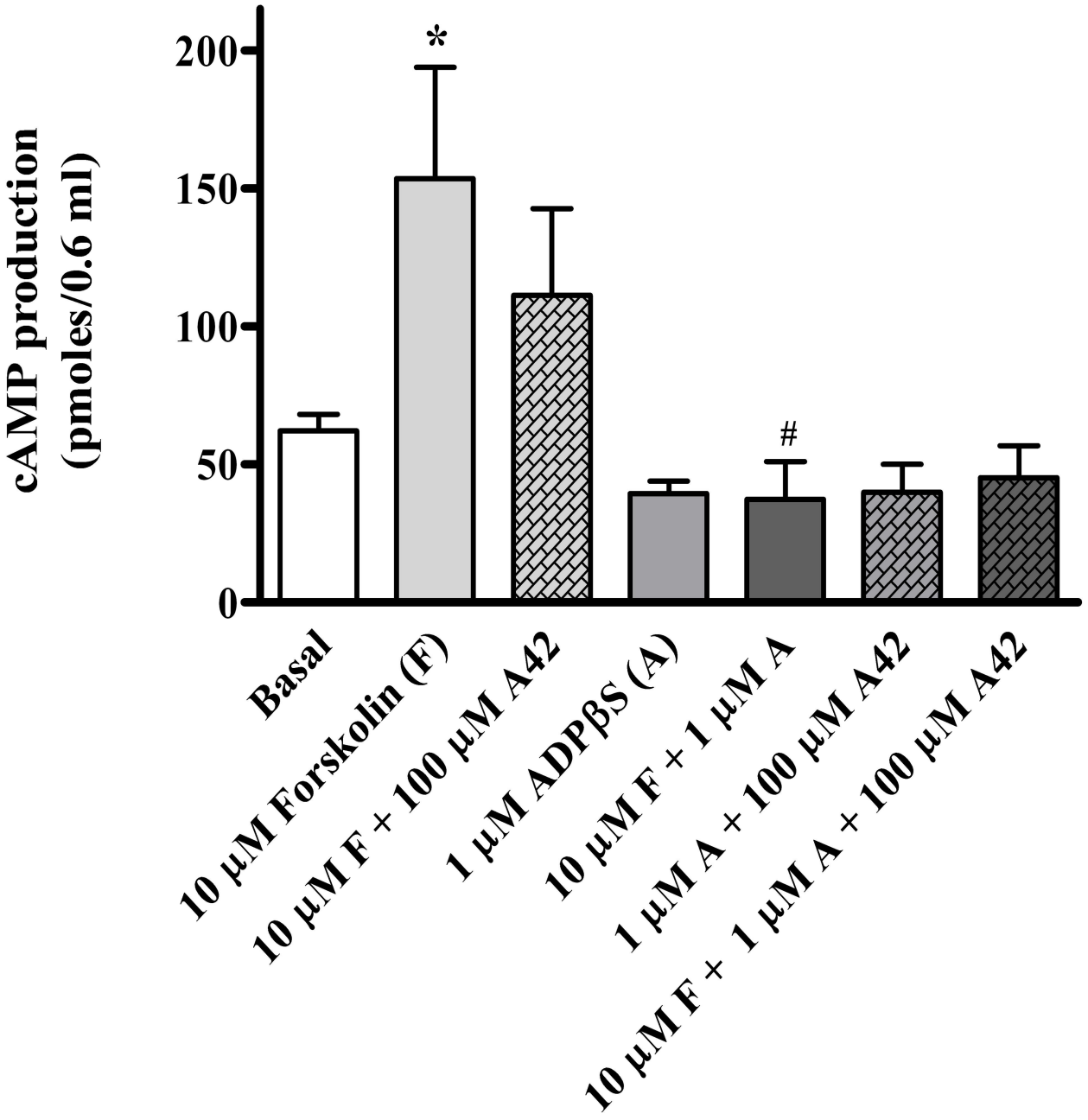

Fig. 4

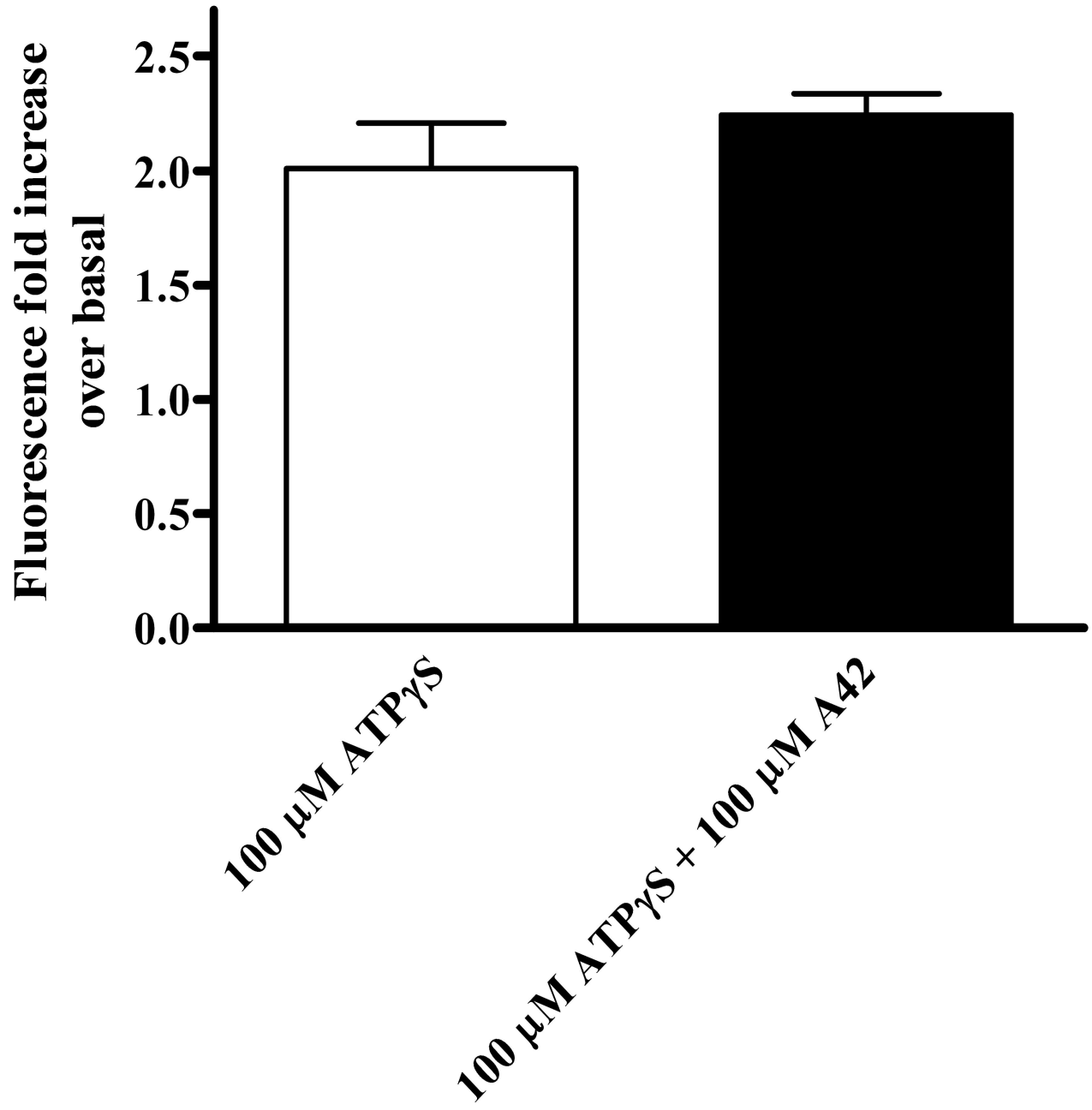

Fig. 5

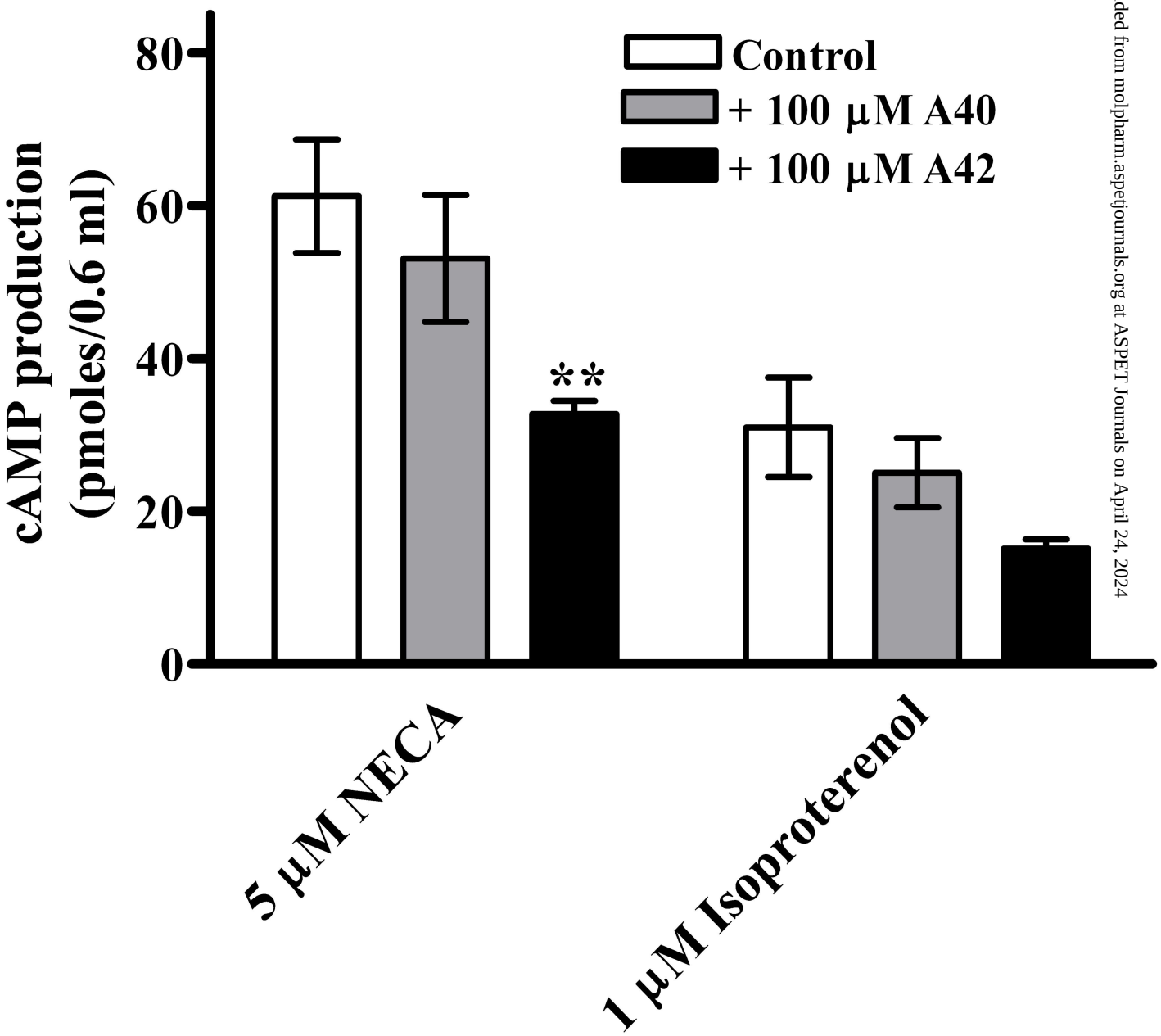

Fig. 6

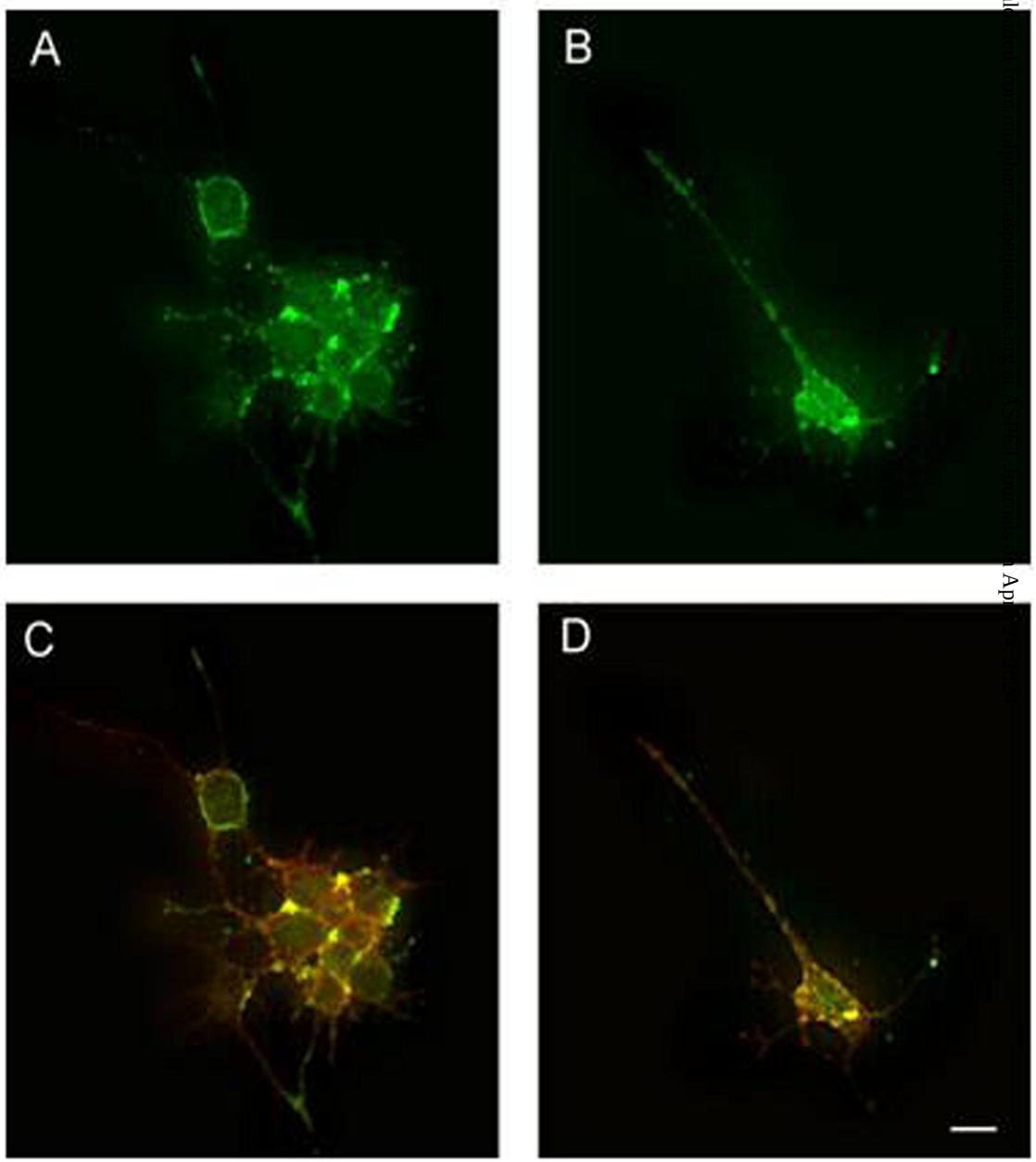

Fig. 7A

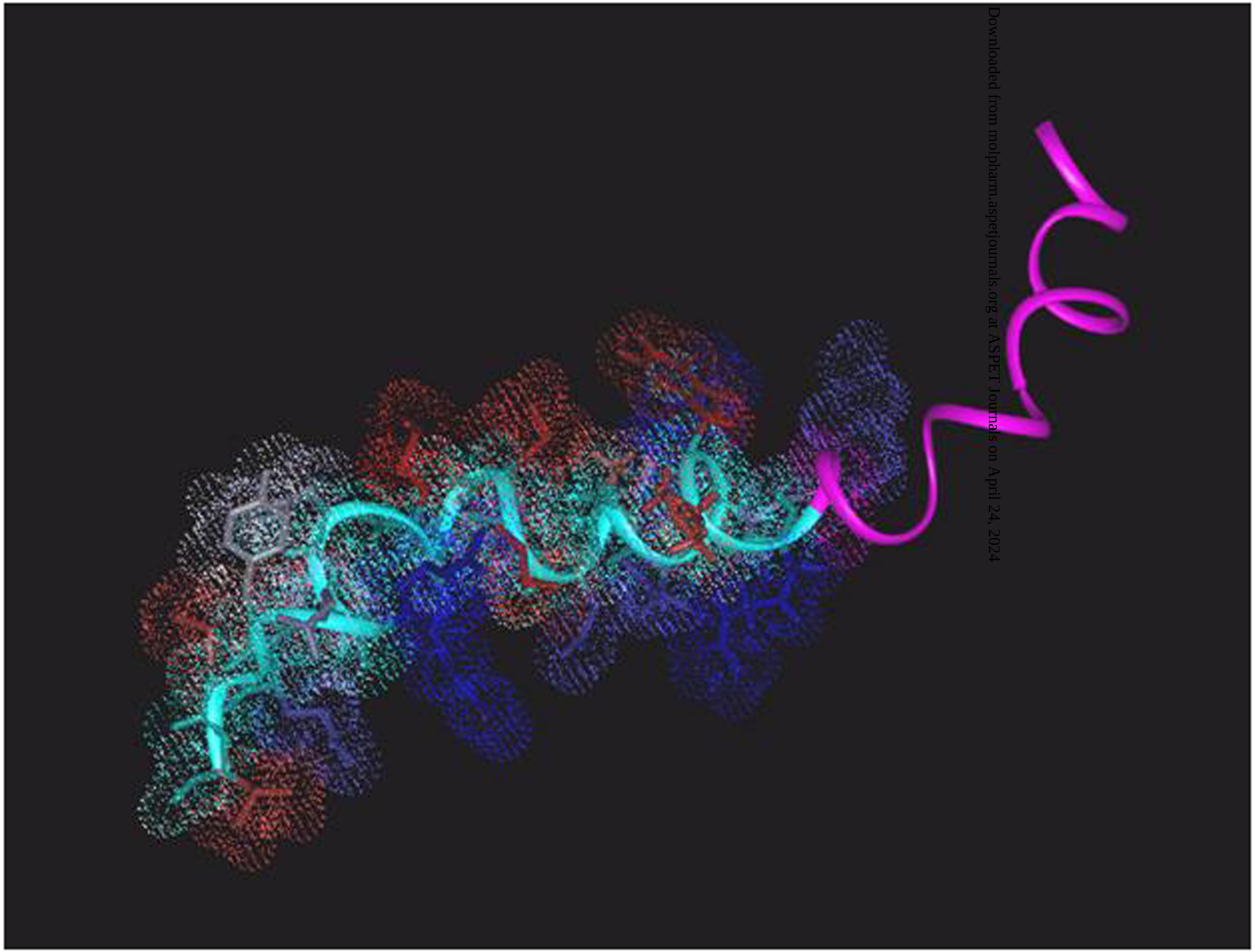

Fig. 7B

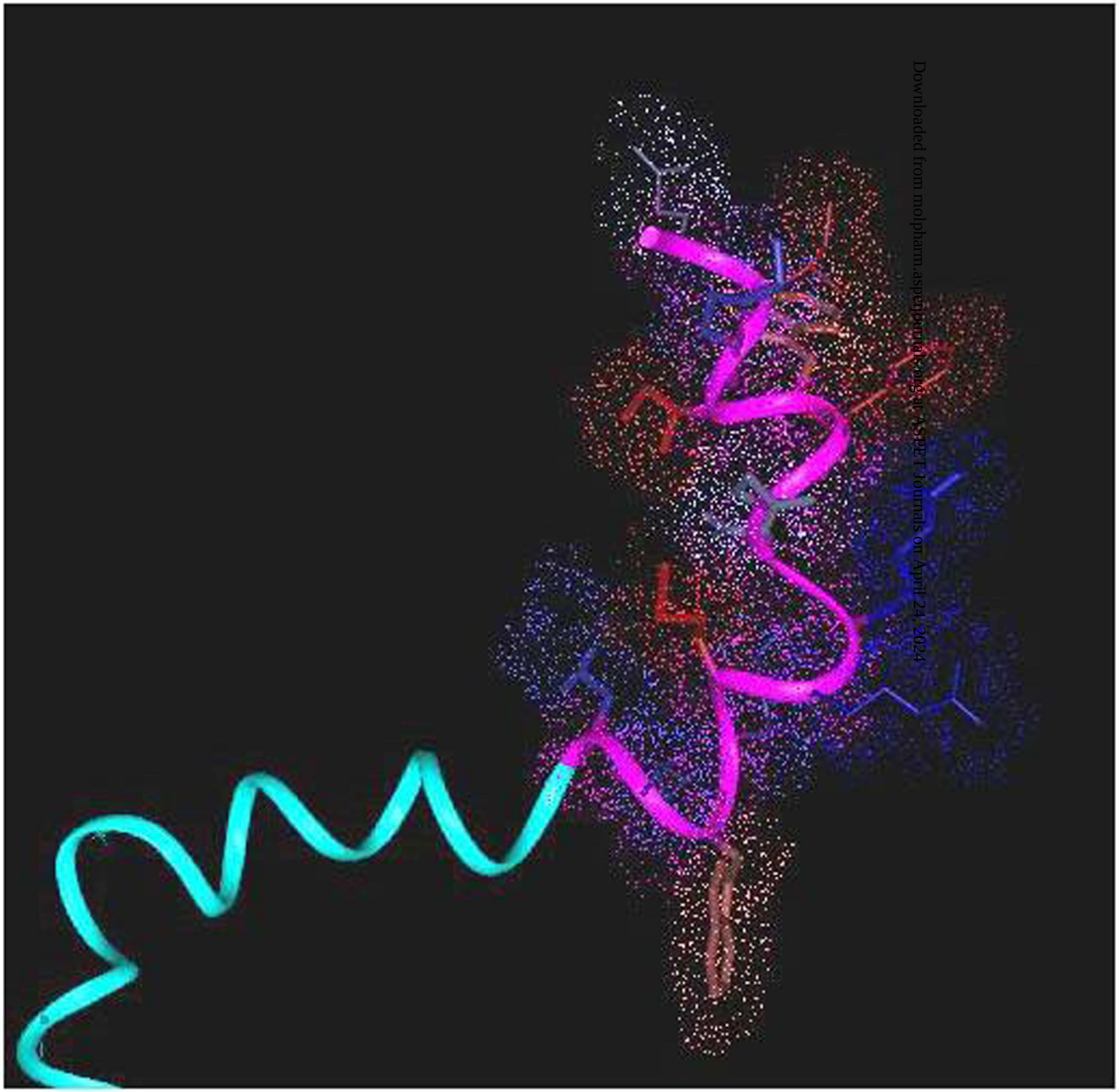

Fig. 8